Masonry panels under in-plane loading: a comparison between experimental and numerical results

U. Andreaus, L. Ippoliti

Dipartimento di Ingegneria Strutturale e Geotecnica, Facoltà di Ingegneria, Università degli Studi di Roma "La Sapienza", Rome, Italy

ABSTRACT

A comparison between experimental and numerical results has been worked out for brick masonry panels under a wide range of biaxial stress states.

The numerical simulation has been carried out via ANSYS code. The single panel has been discretized by means of an eight noded solid element and 3-D incremental analysis has been performed under in-plane loading in order to trace the crack growth and propagation, and to evaluate the ultimate load at failure. Material has been assumed to be linear elastic and to exhibit brittle failure in tension.

In the present paper the brick panel has been modelled in different ways as far as discretization mesh (either macro- and micro-modelling have been adopted) is concerned. A parametric investigation has been worked out in order to identify numerical data which allow the best fitting of experimental results.

1 INTRODUCTION

Performing ultimate analysis of masonry walls via "general-purposes" finite element codes requires material input data to be identified on the basis of experimental results, in order to correctly simulate overall behaviour of structures. Masonry is a composite material consisting of bricks units and mortar joints. Due to the large number of influence factors and the scarcety of experimental results to characterize the mechanical behaviour of the components, attempts made to accurately model this kind of structures are not trivial ones.

On one hand, it is in Authors' opinion that the test series conducted by Page [1], Dhanasekar *et al.* [2], Page [3] on small-size panels prove to be a valuable starting point for such identification procedures; these specimens are

604   Computational Methods and Experimental Measurements

constituted of solid-brick, single-wythe masonry and are subjected to a wide range of biaxial stress states. These tests have been chosen because of the availability of material characteristics, crack patterns at collaspe and failure surfaces, Dhanasekar *et al.* [4], interpolated on the basis of original experimental results. One of the Author examined and classified the collapse mechanisms exhibited by the above mentioned panels, pointing out the main causes of their failure, namely cracking of clay bricks and debonding of mortar joints, Andreaus & Ceradini [7].

On the other hand, the well-known ANSYS code [8] allows to easily deal with many degrees of freedom problems and material nonlinearities, which are often encountered in the analysis of masonry structures; in fact, a solid element is available which is capable of cracking in tension and crushing in compression, and the solution is driven to convergence by means of equilibrium iterations.

Thus, aim of this paper is
- to perform a parametric analysis in order to find out the most significant factors affecting the structural behaviour of masonry panels under biaxial stress states, namely strength characteristics of masonry and of its components;
- to make a comparison between the results obtained by means of different criteria of discretization:

(i) the single finite element comprises an assemblage of units and joints and hence can be characterized by avarage properties of an ideal homogeneous material, i. e. the so-called *macro-modelling*;

(ii) masonry components are separately modelled by finite elements characterized by distinct properties, i. e. the so-called *micro-modelling*;
- to compare the results, namely ultimate load and crack patterns, given by the above mentioned laboratory tests with the output generated by a numerical simulation; and
- to identify input data which allow the best fitting of experimental results, as far as panel failure surfaces are concerned, on the basis of different discretization criteria.

2 SPECIMEN CHARACTERISTICS

Test series have been performed by Page [1], Dhanasekar et a. [2], Page [3] on small-size square panels 0.36x0.36x0.05 m, constituted by brick units 0.11x.0.05x0.035 m. Table 1 shows material properties exhibited by masonry and its components. the bond strength in tension f_{tn} and shear f_s of bed joints (in direction normal to the layers) are given in Page [1]; the Young's modulus E and the Poisson's ratio ν are given in Dhanasekar *et al.* [2]; the tensile $(_t)$ and compressive $(_c)$ strength (f) of masonry in direction normal $(_n)$ and parallel $(_p)$ to the bed joints are given in Page [3], as well as stiffness and strength characteristics of mortar and brick.

Table 1. Material characteristics							
	E [MPa]	ν	f_{tn} [MPa]	f_{cn} [MPa]	f_{tD} [MPa]	f_{cD} [MPa]	f_s [MPa]
mortar	-	-	-	5.08			
brick	7550.	0.167	-	15.41			
joint	-	-	0.13	-			0.30
masonry	5700.	0.190	0.24	7.7	0.40	4.33	0.40

3 FINITE ELEMENT MODEL AND ANALYSIS

The masonry panel has been discretized by means of an eight noded solid element (SOLID65 3-D reinforced concrete solid), ANSYS [8], and an incremental analysis has been performed under in-plane loading in order to trace the crack growth and propagation, and to evaluate the ultimate load at failure.

The most important aspect of this element is the treatment of nonlinear material properties. The solid is capable of cracking in tension (in three orthogonal directions) and crushing in compression and is defined by eight nodes and the isotropic properties. The presence of a crack at an integration point is represented through modification of the stress-strain relations by introducing a plane of weakness in a direction normal to the crack face. Also, a shear transfer coefficient α_t is introduced which represents a shear strength reduction factor for those subsequent loads which induce sliding (shear) across tha crack face. If the crack closes, then all compressive stresses normal to the crack plane are trasmitted across the crack and only a shear strength reduction factor α_c for a closed crack is introduced. Typical shear transfer coefficients range from 0.0 to 1.0, with 0.0 representing a smooth crack (complete loss of shear transfer), and 1.0 representing a rough crack (no loss of shear transfer). This specification may be made for both the closed and open crack.

Material characteristics for failure/cracking/crushing in the ANSYS code are based on an enhanced version of the five parameter failure model, William & Warnke [6]. With the above mentioned algorithm concrete- and rock-like material behaviour can be modelled with a minimum of two parameters, the ultimate tensile strength f_t, and the ultimate compressive strength f_c. The other three parameters that may be used are experimental values for biaxial crushing stress f_{cb}, biaxial crushing under ambient hydrostatic stress f_1, and uniaxial crushing stress under ambient hydrostatic stress state f_2. In this work two parameters f_t and f_c has been assigned while for the other three parameters f_{cb}, f_1 and f_2 default values $f_{cb} = 1.2 f_c$, $f_1 = 1.45 f_c$, $f_2 = 1.725 f_c$ have been assumed. The criterion for failure due to a multiaxial stress state can be expressed in the form:

$$F/f_c - S \geq 0, \tag{1}$$

606   Computational Methods and Experimental Measurements

where:

F = a function of the principal stress state,

S = a failure surface expressed in terms of principal stresses and five input parameters f_t, f_c, f_{cb}, f_1 and f_2,

f_c = uniaxial crushing strength.

If eqn. (1) is not satisfied, there is no attendant cracking or crushing. Otherwise, the material will crack if any principal stress is tensile while crushing will occur if all principal stresses are compressive.

Masonry joints exhibit extremely low dilatancy; thus, according to concluding remarks of Dhanasekar *et al.* [5], material's stress-strain relationship has been assumed to be linearly elastic and brittle either in tension and compression, which is the cause of nonlinear structural behaviour. One approach to nonlinear solutions involves breacking the load into a series of load increments. The load increments can be applied either over several load steps or over several substeps whitin load step. At the completion of each increment solution, the program adjusts the stiffness matrix to reflect the non linear changes in structural stiffness, before proceeding to the next load increment.

The masonry panel has been subjected to biaxial stress states at different values of compressive normal stress in direction parallel to be joints $\sigma_p = 0.0$, -1.0, -2.0, -4.0 MPa, and the ultimate shear stress has been evaluated at collapse.

4 MACRO-MODELLING

The masonry panel has been assumed to exhibit average homogeneous properties and has been discretized by means of 5x6=30 elements 0.072x0.06x0.05 m; the element size is such that it comprises one half of an assemblage constituted by two bricks and the intervening bed joint; therefore, non uniform stress distribution along the bed joints can be considered. A sensitivity analysis performed on mesh density stated that the adopted mesh refinement is the lower bound for the objectivity of ultimate load. The solid element of Sect. 3 is defined by the isotropic properties shown in Table 2.

Table 2. Material properties in macro-modelling.						
	E [MPa]	ν	f_t [MPa]	f_c [MPa]	α_t	α_c
masonry	5700.	0.19	1.0	8.0	1.0	1.0

5 MICRO-MODELLING

The masonry panel has been considered as an assemblage of brick units 0.11x.0.05x0.035 m. and mortar layers (bed and head joints) 0.01 m thick; the single components are defined by the isotropic properties shown in Table 3.

Table 3. Material properties in micro-modelling.						
	E [MPa]	ν	f_t [MPa]	f_c [MPa]	α_t	α_c
brick	7550.	0.167	1.	15.41	1.	1.
mortar	3000.	0.2	0.4	5.08	1.	1.

6 CONCLUSIONS

Figures 1, 2, 3, 4 illustrate the comparisons between numerical and experimental failure curves. In the case σ_p=-2.0, σ_n=-2.0 the equilibrium path has been traced up to failure in Fig. 5, and the crack pattern depicted in Fig. 6, where black colored zones denote crack opening.

Generally speaking, as far as ultimate loads, crack distribution, and equilibrium path, numerical and experimental results show a good agreement, as well as macro- and micro-modelling results. More in detail, tensile strength and shear transfer coefficients have revealed to be the "key" parameters. In order to numerically generate failure surfaces which reproduce with sufficient accuracy the experimental ones, macro-modelling required to adopt a tensile strength for the solid element much larger than that one obtained for masonry material by laboratory tests.

Brick cracking and joint debonding can be directly represented, while spalling in the middle plane can be indirectly obtained by the comparison between lateral strain due to Poisson's effect and brick ultimate strain.

7 REFERENCES

1. Page, A. W. The Biaxial compressive strength of brick masonry, *Proc. Instn. Civ. Engrs.*, 1981, **71**, 893-906.
2. Dhanasekar, M., Page A. W. & Kleeman P. W. The elastic properties of brick masonry, *Int. J. Mas. Constr.*, 1982, **2**, 4, 155-160.
3. Page A. W. The strength of brick masonry under biaxial tension-compression, *Int. J. Mas. Constr.*, 1983, **3**, 1, 26-31.
4. Dhanasekar, M., Page, A. W. & Kleeman, P. W. The failure of brick masonry under biaxial stresses, *Proc. Instn. Civ. Engrs.*, 1985a, **79**, 295-313.
5. Dhanasekar, M., Kleeman, P. W. & Page A. W. Biaxial stress-strain relations for brick masonry, *J. Struct. Div.*, ASCE, 1985b, **111**, 5, 1085-1100.
6. William, K. J. & Warnke, E. D. Constitutive model for the triaxial behaviour of concrete, Ed. ISMES, **19**, 174, *Proc. IABSE*, Bergamo, Italia, 1975.
7. Andreaus, U. & Ceradini, G. Failure modes of solid brick masonry under in-plane loading, *Masonry International*, 1992, **6**, 1, 4-8.
8. ANSYS Engineering Analysis System, *Theoretical and User's Manuals*, Revision 5.0, Swanson Analysis System Inc., Houston, 1992.

608 Computational Methods and Experimental Measurements
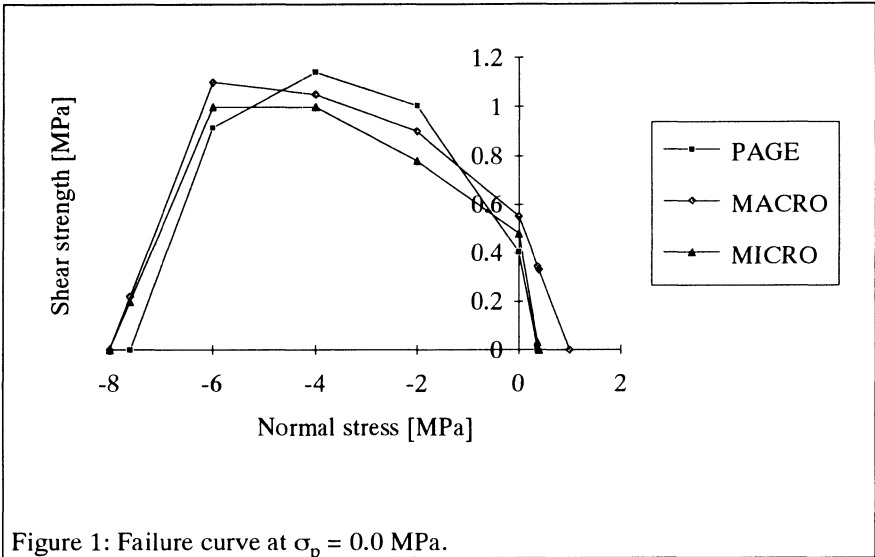
ACKNOWLEDGEMENTS

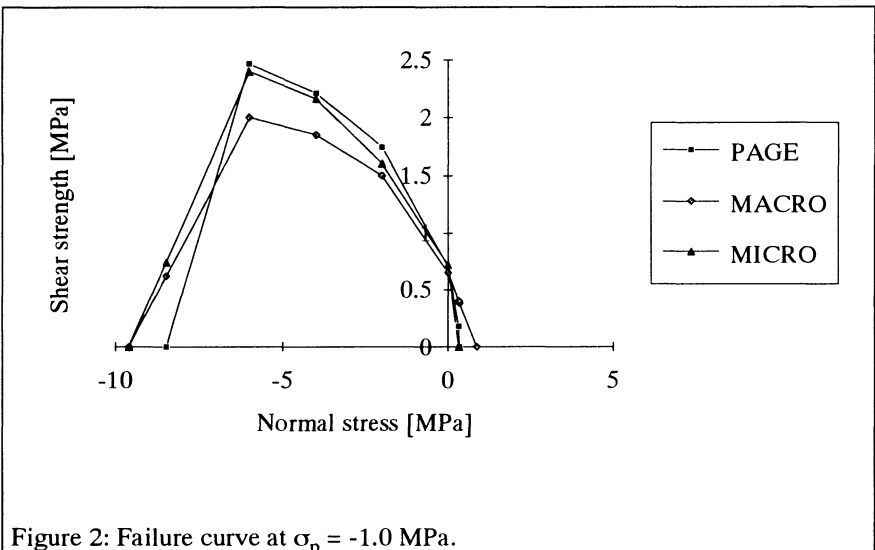Figure 1: Failure curve at σ_n = 0.0 MPa.

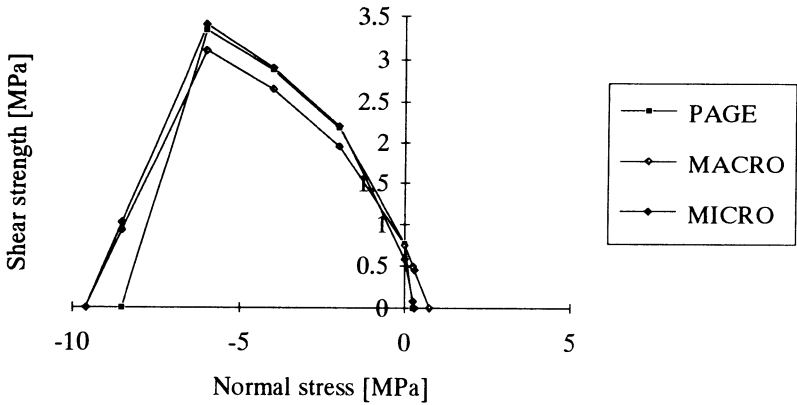Figure 2: Failure curve at σ_n = -1.0 MPa.

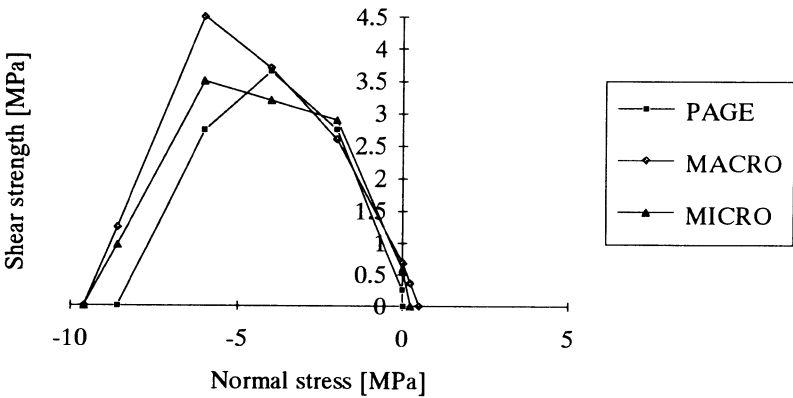Figure 3: Failure curve at σ_p = -2.0 MPa.

Figure 4: Failure curve at σ_p = -4.0 MPa.

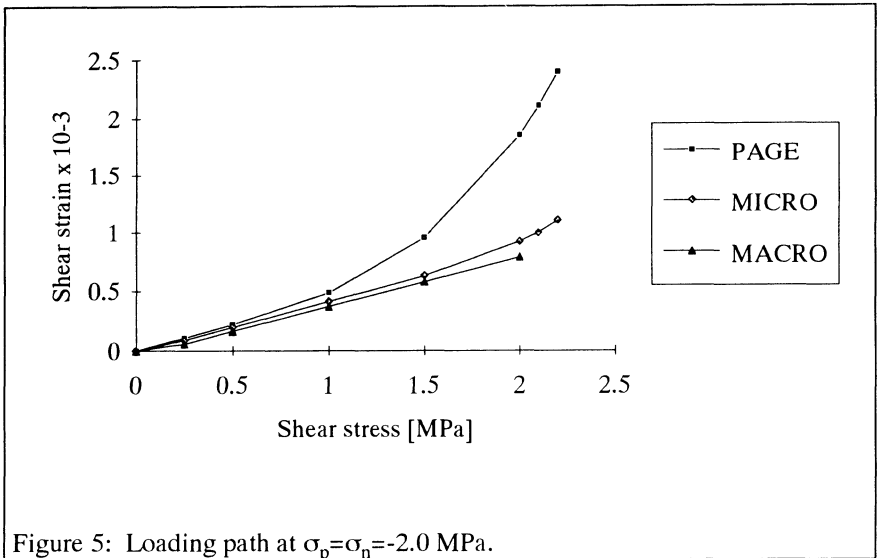610   Computational Methods and Experimental Measurements

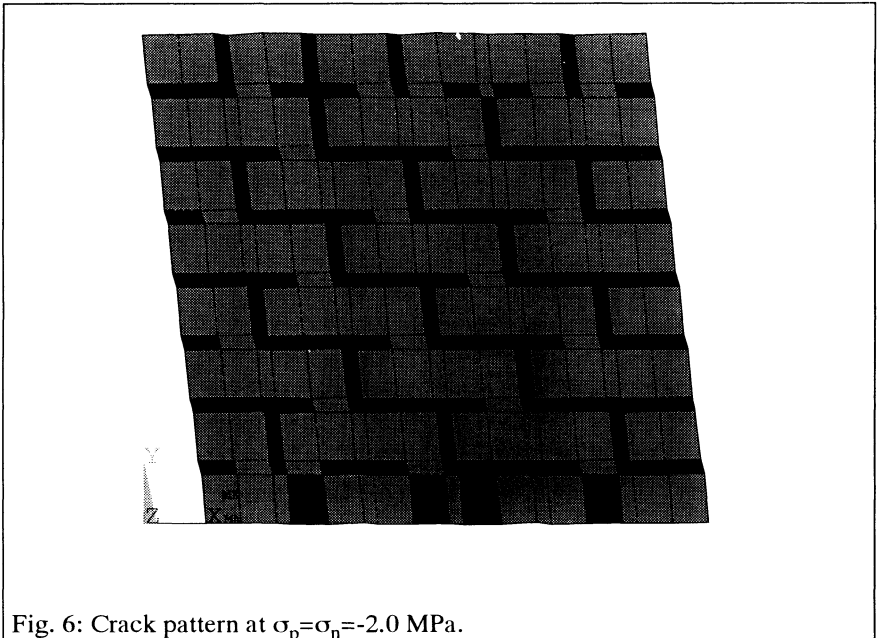Figure 5: Loading path at $\sigma_p = \sigma_n = -2.0$ MPa.

Fig. 6: Crack pattern at $\sigma_p = \sigma_n = -2.0$ MPa.